CYBERNETICS AND PHYSICS, VOL. 8, NO. 3, 2019, 106–113

NEURONAL PATHWAY AND SIGNAL MODULATION FOR MOTOR COMMUNICATION

Parth Chholak
Center for Biomedical Technology
Technical University of Madrid
Spain
parth.chholak@ctb.upm.es

Alexander N. Pisarchik
Center for Biomedical Technology
Technical University of Madrid
Spain
alexander.pisarchik@ctb.upm.es

Semen A. Kurkin, Vladimir A. Maksimenko, Alexander E. Hramov
Research and Educational Center 'Artificial Intelligence Systems and Neurotechnology'
Yuri Gagarin State Technical University of Saratov
Russia
kurkinsa@gmail.com, maximenkovl@gmail.com, hramovae@gmail.com

Article history:
Received 17.09.2019, Accepted 26.11.2019

Abstract

The knowledge of the mechanisms of motor imagery (MI) is very important for the development of brain-computer interfaces. Depending on neurophysiological cortical activity, MI can be divided into two categories: visual imagery (VI) and kinesthetic imagery (KI). Our magnetoencephalography (MEG) experiments with ten untrained subjects provided evidences that inhibitory control plays a dominant role in KI. We found that communication between inferior parietal cortex and frontal cortex is realised in the mu-frequency range. We also pinpointed three gamma frequencies to be used for motor command communication. The use of artificial intelligence allowed us to classify MI of left and right hands with maximal classification accuracy using the brain activity encoded in the identified gamma frequencies which were then proposed to be used for communication of specifics. Mu-activity was identified as the carrier of gamma-activity between these areas by means of phase-amplitude coupling similar to the modern day radio wave transmission.

Key words

Brain-computer interface, motor imagery, inhibition, neural communication, phase-amplitude coupling, inferior parietal.

1 Introduction

Brain-computer interfaces (BCI) aim to control external devices as per the interpretation of the operator's brain activity [Abiri et al., 2019]. BCI systems can be classified into two general categories [Abiri et al., 2019]. In the first category, feedforward brain activity is used to control external devices, and in the second category, closed-loop brain activity with feedback device(s) is used for neural rehabilitation.

The important task of BCI applications is the recognition of the patterns of neurophysiological brain activity associated with motor imagery (MI) which is defined as a mental simulation of overt actions in the absence of any muscle movements. This bears crucial importance for both brain-controlled exoskeletons or bioprosthesis and neurorehabilitation of amputee and stroke patients. MI can be classified into two categories, namely, visual imagery (VI) and kinesthetic imagery (KI) [Chholak et al., 2019]. While in VI subjects MI activates visual cortex, in KI subjects the activity is detected in the same motor areas as in the case of real movements [Pfurtscheller and Neuper, 1997] with an additional mechanism for inhibiting motor commands to avoid overt actions ([Solodkin et al., 2004]; [Hanakawa et al., 2008]; [Guillot et al., 2012]; [Abiri et al., 2019]). Functional magnetic resonance imaging (fMRI) studies evidence the involvement of motor associated areas and inferior parietal (IP) cortex for KI subjects, in contrast to VI subjects who exhibit the involvement of visual and superior parietal cortices [Guillot et al., 2009]. Moreover, transcranial magnetic stimulation (TMS) experiments suggest that the IP area participates in the inhibitory control of the precentral gyrus (PCG) during KI-dominated MI [Lebon et al., 2012]. However, despite extensive research on MI, no

clear experimental evidence of the underlying KI mechanism has yet been provided.

One of the most popular experimental paradigms for MI studies is based on sensorimotor rhythms (SMR) [Abiri et al., 2019], which involves KI of large body parts, such as whole limbs, to obtain modulations of neuronal activity [Morash et al., 2008]. At the same time, alpha- and beta-rhythms are crucial and ubiquitous in most studies on MI [Craik et al., 2019]. For example, in 1991 [Wolpaw et al., 1991] used the alpha-rhythm to control the cursor position on a computer screen in one-dimensional space. Later, more advanced and sophisticated methods, such as linear regression, logistic regression, and artificial neural networks (ANNs), were applied to control the cursor position in three-dimensional space ([Wolpaw and McFarland, 2004]; [Wolpaw and McFarland, 1994]; [McFarland et al., 2010]), prosthetics ([Murguialday et al., 2007]; [Chen et al., 2008]; [Ramos-Murguialday et al., 2013]), robots ([Müller-Putz et al., 2005]; [Kai Keng Ang et al., 2009]; [Sarac et al., 2013]; [Baxter et al., 2013]; [LaFleur et al., 2013]), and for stroke rehabilitation [Ramos-Murguialday et al., 2013]; [Ono et al., 2014]; [Rayegani et al., 2014]) (for review see [Abiri et al., 2019] and [Ang et al., 2012]).

Among the massive amount of literature on the BCI development using MI, electroencephalography (EEG) is found to be the most popular noninvasive technique ([Bi et al., 2013]; [Machado et al., 2013]; [Moghimi et al., 2013]; [Vaughan et al., 1996]; [Hwang et al., 2013]; [Lotte et al., 2007]; [Pfu, 2006]; [Machado et al., 2010]) for controlling wheelchairs [Bi et al., 2013], communication aid systems [Birbaumer et al., 1999], assistive and rehabilitative devices for healthy [Meng et al., 2016] and disabled people, stroke patients and people with other neurological deficits ([Daly and Wolpaw, 2008]; [Birbaumer and Cohen, 2007]; [Machado et al., 2013]; [Moghimi et al., 2013]; [Birbaumer, 2006]). In addition, a fair amount of papers were devoted to magnetoencephalography (MEG) studies on MI ([Salmelin and Hari, 1994]; [Schnitzler et al., 1997]; [Kauhanen et al., 2004]; [Halme and Parkkonen, 2016]; [Halme and Parkkonen, 2018]), which has the advantage of a higher spatial resolution and better resilience against artifacts as compared to EEG, although pros of EEG, such as low cost and portability, are crucial for BCI development, but can be kept aside while understanding the fundamental activity underlying MI.

The aim of this study is to analyse MEG signals, especially in the alpha- and beta-frequency bands, associated with MI in the SMR paradigm. We focus on the inhibitory mechanism to avoid overt action during KI, that was previously investigated using other neuroimaging techniques, such as TMS. Subsequently, we perform various validation tests along the way using methods based on spectral power, coherence and artificial neural networks (ANN), and suggest a model which explains empirical observations related to KI and real movements (overt actions).

2 Materials and Methods

The neurophysiological data were acquired using the Vectorview MEG system (Elekta AB) with 306 channels (102 magnetometers and 204 planar gradiometers) placed inside a magnetically shielded room (Vacuum Schmelze GmbH). Three fiducial points (nasion, left and right preauricular) were acquired for each subject.

The experimental study consisted of ten (eight males) previously *untrained* volunteers between the age of 20 and 31. The subjects sat in a comfortable reclining chair with their legs straight, shoes off, and arms resting on an armrest in front of them. All of them provided a written informed-consent before the experiment commencement. The experimental studies were performed in accordance with the Declaration of Helsinki.

Spatiotemporal signal space separation of [Taulu and Hari, 2009] was used to separate neuronal signals from nearby electromagnetic interference. The signals from bad MEG channels were replaced with spatially-averaged signals of the nearby well-functioning MEG channels. The software used for this preprocessing task was MaxFilter that came along with the Elekta-Neuromag machine. The sampling frequency was 1000 Hz and an online anti-alias [0.1–330] Hz bandpass filter was utilised.

The experimental protocol was designed as follows. Resting-state recordings were performed at the start and end of each experiment with open eyes (OE) and closed eyes (CE), respectively. OE recordings were later discarded because all data during MI were recorded with closed eyes. The duration of CE recordings was different for each subject and ranged from 40 to 280 s. The recordings were divided into four series sets. Every series contained the MEG data of MI of each of four limbs in a random order, i.e., left hand (LH), right hand (RH), left leg (LL), and right leg (RL). Before MI of each limb, a visual message was demonstrated to the subject to ask him/her to close eyes and imagine the movement of the indicated limb as soon as he/she hears a beep. The subsequent beeps were made every 6–8 s (the time interval was ordered randomly). Each imaginary movement between the beeps was counted as one trial. The number of trials for each limb was varied among subjects between 4 and 7 in each series. After every series, the subjects had a 40-s rest during which they listened to a relaxing music.

The experiments were programmed using software provided by the Cogent 2000 team at the Functional Imaging Laboratory and the Institute of Cognitive Neuroscience and Cogent Graphics developed by John Romaya at the Laboratory of Neurobiology at the Wellcome Department of Imaging Neuroscience. A MATLAB code was used to produce all audio and visual commands (Cogent) as well as to log the time at the beginning of each MI-trial in a protocol file (in .txt format). The protocol file was later used to mark all events

manually when analysing the MEG file (in .fif format). A part of the data analysis was performed with Brainstorm [Tadel et al., 2011] documented and freely available for downloading under the GNU general public license (http://neuroimage.usc.edu/brainstorm). Once the beginnings of each limb's MI were marked using the protocol file, 5-s trials were extracted immediately following these marks. Similarly, 10-s trials from CE recordings were also marked and extracted as the background activity for every subject.

The time-frequency structure of the MEG signals was analysed with the help of a wavelet-based approach, well-known for the analysis of nonstationary time-series in medicine and biology [Iva, 1999]. For each limb, we used Morlet wavelets with $f_0 = 1$ Hz central frequency and a 3-s full width at half maximum to evaluate time-frequency spectrograms (TFS) for all extracted 5-s MEG-trials of each limb, and then averaged the TFS to all trials for that limb. Then, the TFS was also averaged over desired frequency ranges of delta (1–5 Hz) and mu (8–30 Hz). The same process was repeated for the background 10-s trials using the same parameters. To evaluate event-related synchronisation/desynchronisation (ERS/ERD), we took the difference between the spectrogram for the MI-trials and the averaged-over-time spectrogram of the background and then normalized it to the background. This normalized difference was assumed to be positive for ERS and negative for ERD.

Magnitude squared coherence was used as a measure of connectivity between two brain regions. After modelling the brain using a mesh of about 15000 vertices, the observed brain activity in the 306 MEG channels was mapped onto the brain sources situated at these vertices using additional constraints such as minimisation of total system energy. The effects of depth-dependent sensitivity and spatial resolution were normalised using the sLORETA method. Desikan-Killany atlas in Brainstorm [Tadel et al., 2011] was used to identify vertices corresponding to the IP and PCG, and subsequently average responses of these regions were evaluated for coherence studies.

ANN were used in the later stages for validation purposes. Multilayer perceptron (MLP) was chosen as the network architecture to classify between LH and RH MI-trials. The input data for the ANN were taken from MEG time series from all 102 magnetometers, after bandpass filtering with a 10-Hz passing window. This passing window was varied from 5–60 Hz in steps of 5 Hz, i.e., (5–15), (10–20), (15–25), ..., and (50–60) Hz. The input layer containing 102 neurons was followed by three hidden layers having 30, 15 and 5 neurons, respectively. The output layer consisted of a single neuron. A scaled conjugate gradient training algorithm was used. The training stopped as soon as the batch training with all input data ran for at least 5000 times. To improve the efficiency of machine learning, we randomly mixed the input signal maintaining the correspondence to the MI-type, either LH or RH. Therefore, to classify MI of LH and RH, we mixed the MEG time series of all collected trials related to the LH and RH for each channel without losing their corresponding targets (0 for LH and 1 for RH) and time instance. The ANN classification was carried out in MATLAB (R2017a; Mathworks Inc., MA, USA) using Neural Network Toolbox.

3 Results and Discussion

Based on differential μ-activity of the cortex, we first segregated the subjects into two groups, six KI subjects (Sub 1, 2, 4, 5, 9 and 10) and four VI subjects (Sub 3, 6, 7 and 8). The differentiation was performed according to ERS/ERD. Specifically, the KI subjects exhibited ERD in the aforementioned associated cortical sites, while the VI subjects showed ERS. Curiously, [Pfurtscheller and Lopes da Silva, 1999] reported event-related desynchronisation (ERD) of μ-rhythms in the discussed KI sites during MI in the SMR paradigm and ERS for resting. Although the subjects in our study were instructed to perform KI, only some of them could successfully achieve this goal, because all participants were *untrained*.

The obtained results are in agreement with the previous study, where KI subjects (successful-SMR) exhibited ERD in μ-band, while VI subjects (failed-SMR) showed ERS, similar to the resting state of SMR. In the δ-range, all KI subjects exhibited either ERS or ERD in the frontal cortex and insignificant activity in the posterior parts of the brain. On the other hand, the VI subjects exhibited the distributed non-uniform activity without any preference for a particular region. The method used to evaluate ERS/ERD was as explained in section 2.

As discussed in section 1, KI and real movements share a common neuronal network, distinctly to KI which involves an additional mechanism for inhibiting overt movement that is likely to be situated in the IP. The coincidence of finding ERD for the KI subjects in μ-band at the same site as the one that is responsible for inhibitory control (i.e., IP) instils curiosity and deems to be further looked upon. In order to reveal the mechanism underlying this inhibitory control, we suppose that desynchronised activity of neurons near the IP disrupts signal propagation that passes from IP to PCG, as hinted by TMS studies.

[Sirigu et al., 1996] showed that when subjects were asked to predict beforehand the time necessary to perform motor tasks, the subjects with lesions in the posterior parietal cortex typically underestimated/overestimated the time. This strongly contrasted with subjects having dysfunctional motor regions who exhibited impaired movements, but retained the ability to estimate motor performance times [Sirigu et al., 1995]. Prefrontal cortex (PF) is also known to be involved in inhibition of movements (Krams et al, 1998), more specifically in choosing between the responses (Duque et al, 2012).

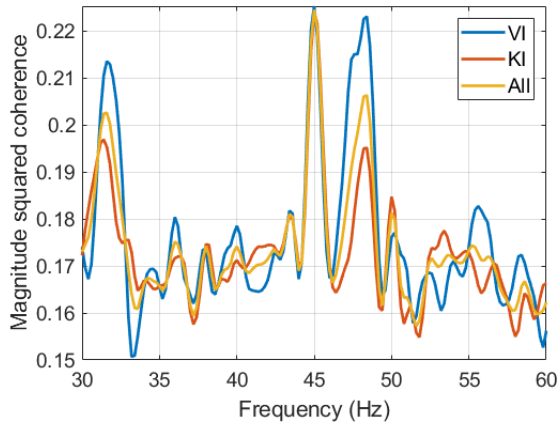

Figure 1. Connectivity between IP and PCG for both MI groups and all subjects together. Gamma range peaks were obtained at 32-Hz, 45-Hz, and 48-Hz.

In order to predict motor performance times, a subject needs to simulate the entire repertoire of the act from long-term memory. This function is perhaps localised in the posterior parietal cortex. Conveniently, nearby temporal lobe has been implicated to play a role in long-term memory function, especially the medial temporal lobe [for review see [Jeneson and Squire, 2012]]. Before the actual execution of motor commands by M1, aided by its associated areas like premotor cortex (PM) and supplementary motor area (SMA), passable responses are likely to be chosen at PF. As most of the conscious processing is performed in the frontal cortex, PF being the point hosting this decision-making process is amenable.

We therefore propose the following neuronal pathway for motor signals. Motor commands are generated in the posterior parietal cortex and need to travel to PF before being relayed to motor associated areas for final execution. ERD centred around IP disrupts the communication of motor commands from the posterior parietal cortex to frontal cortex in order to avoid any overt movement during KI.

[Schwoebel et al., 2002] showed that bilateral lesions in the parietal cortex led to the execution of motor commands during MI experiments without the patient realising it. The patient with lesions at IP may not have ERD in IP at μ-frequency and would pass the signal to the PF region, not expecting an input from IP during KI and thus leading to actual execution without the subject's knowledge. At the same time, injured parietal cortex would also ensure no feedback of the movement through the sensory system.

The coherence results indicate better communication in the μ-band between IP and PCG for VI subjects in comparison to KI subjects who show a clearly compromised connectivity between these areas. We plot the mean-squared coherence of the MEG signals collected from IP and PCG versus frequency (in Hz) in γ-band range. Apart from a peak at 10-Hz μ, the strength of connectivity between IP and PCG showed peaks at 32-, 45-, and 48-Hz gamma frequencies for both groups of subjects (Fig.1). ([Bressler, 1995]; [Varela et al., 2001]; [Fries, 2005]; [Siegel et al., 2012]) also validate that coherence in γ-band between two points of the brain can be used to control neural communication of information between them.

[Lisman and Jensen, 2013] discussed about a theta-gamma neural code for multi-message communication during memory processes. They prescribed phase-amplitude coupling between the phase of θ-waves and the amplitude of γ-waves and envisaged upon the extension of their model to sensory processes if θ-waves are replaced by μ-waves. The studies of ([Llinás and Ribary, 1993]; [Mormann et al., 2005]; [Canolty et al., 2006]; [Demiralp et al., 2007]; [Sauseng et al., 2009]; [Axmacher et al., 2010]; [Voytek et al., 2010]; [Maris et al., 2011]) provide evidences of this phase-amplitude coupling in humans. During each γ-cycle, a set of neurons or neural ensemble fire concurrently, forming a spatial pattern on the cortex that corresponds to the object being represented by that γ-cycle. ([Skaggs et al., 1996]; [Harris et al., 2003]; [Dragoi and Buzsáki, 2006]; [Gupta et al., 2012]) showed that a sequence of generated information in the form of gamma-cycles gets mapped to different phases of theta wave, maintaining the same order of information generation. [Voytek et al., 2010] have reported shifts in gamma phase-amplitude coupling frequency from theta to alpha during visual tasks. Similarly, we expect a phase-amplitude coupling between γ-waves and α- / μ-waves for MI tasks.

We therefore propose that motor commands involve μ-waves as general carriers of motor related activity. These carrier waves carry γ-waves, containing specifics of motor activity from IP to PF, which acts as a relay junction and transfers the information to motor related areas around the PCG.

Our ANN classification study designed in an unconventional yet appropriate way, supports this hypothesis. The study was designed to find what frequency component of the MEG signal generates higher ANN accuracy in order to gauge the kind of ANN classification-task related information carried by that component. As discussed in section 2, bandpass filtering in windows of a 10-Hz width was used to pre-process MEG data before ANN classification of LH and RH MI. ANN classification accuracy was found to be largely independent of the KI or VI mode of MI. Figure 2 shows the ANN classification accuracy averaged over all subjects versus the bandpass frequency range. Each data point in this figure represents the centre of the corresponding bandpass frequency range. Thus, the points at the two local maxima represent 25–35 Hz and 45–55 Hz windows, respectively. Observing the two maxima in the frequency ranges which include the gamma signal frequencies shown in Fig. 1 validates our hypothesis that specifications of MI (e.g., hand motion) were encoded in the γ-band signals. On the other hand, the μ-band

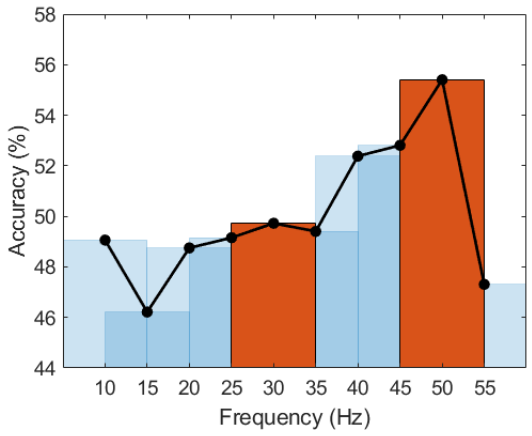

Figure 2. ANN classification accuracy between LH and RH MI averaged for all subjects versus bandpass-frequency range on the input MEG signal to the ANN. Each data point on the x-axis represents the centre of the bandpass-frequency range of a 10-Hz width. Two local maxima in the gamma range are found that coincide the coherence study.

played a general role in this motor task and did not contribute as much in differentiating between two hands. The amplitude of intracellular spiking in γ-band in the directionality-specific (LH or RH) neurons is codependent on the phase of the μ-band signal at 10 Hz which acts as an envelope for motor-related activity between these regions.

In the very recent, systematic and extensive review, [Craik et al., 2019] described only eight studies that employed MLP for deep neural network classification using EEG, three of which were focussed on MI. Only one of these MI studies utilised MEG time series as inputs for ANN [Sturm et al., 2016] with a 75% accuracy, whereas other two studies ([Yohanandan et al., 2018]; [She et al., 2019]) used different forms of frequency transformations on the input signal and achieved up to 85% accuracy. The maximum accuracy obtained in our study, utilising MEG signals as input, was about 85% in the 40–50 Hz range. This means that the physiological information gained out of this study can greatly benefit the efficiency of cybernetic systems such as brain-computer interfaces and at the same time elucidate upon how neuronal communication is parallel to the modern day radio communication.

Future directions for this research can be to verify and quantify phase-amplitude coupling using the mean vector length method suggested by [Canolty et al., 2006]. It would also be interesting simulate the identified network using popular neuronal oscillators such as Hindmarsh-Rose to see the parameters of coupling that can produce complex patterns of collective behaviour as has been done in [Hizanidis et al., 2015].

4 Conclusion

In this work we identified the neuronal pathway for motor command propagation during both kinesthetic imagery and real movements. We also revealed parts of the encoding details and signal disruption to avoid overt action. During KI, desynschronised neurons prevent brain activity in gamma (32-, 45-, and 48-Hz) carrying specifics of the movement to propagate from inferior parietal lobe to the prefrontal cortex which can blindly relay the signal to the motor areas for execution. All motor related communications are performed in the mu (10-Hz) frequency regime using phase-amplitude coupling. Delta waves also participate in this circuit and definitely play an important role in the frontal cortex. We aspire that the identification of these motor related frequencies and the areas in which they are communicated through will turn out to be radical in developing BCIs henceforth. And, the insights about neural communication and inhibition may benefit research on controlling human inhibition towards harmful substances or preventing the propagation of undesirable sensations like pain.

Acknowledgements

This work was supported by the Spanish Ministry of Economy and Competitiveness under Project SAF2016-80240. The data analysis was supported by the Russian Science Foundation (Grant No. 19-12-00050).

References

(1999). *Wavelets in Physics*, chapter Wavelets in medicine and physiology. Cambridge Univ. Press.

(2006). *Encyclopedia of Biomedical Engineering*, vol. 2, chapter EEG based brain–computer interface system, pp. 1156–66. New Jersey: John Wiley and Sons, 1 edition.

Abiri, R., Borhani, S., Sellers, E. W., Jiang, Y., and Zhao, X. (2019). A comprehensive review of EEG-based brain–computer interface paradigms. *Journal of Neural Engineering*, **16** (1), pp. 011001.

Ang, K. K., Chin, Z. Y., Wang, C., Guan, C., and Zhang, H. (2012). Filter Bank Common Spatial Pattern Algorithm on BCI Competition IV Datasets 2a and 2b. *Frontiers in neuroscience*, **6**, pp. 39.

Axmacher, N., Henseler, M. M., Jensen, O., Weinreich, I., Elger, C. E., and Fell, J. (2010). Cross-frequency coupling supports multi-item working memory in the human hippocampus. *Proceedings of the National Academy of Sciences of the United States of America*, **107** (7), pp. 3228–33.

Baxter, B. S., Decker, A., and He, B. (2013). Noninvasive control of a robotic arm in multiple dimensions using scalp electroencephalogram. In *2013 6th International IEEE/EMBS Conference on Neural Engineering (NER)*, IEEE, nov, pp. 45–47.

Bi, L., Fan, X.-A., and Liu, Y. (2013). EEG-Based Brain-Controlled Mobile Robots: A Survey. *IEEE Transactions on Human-Machine Systems*, **43** (2), pp. 161–176.

Birbaumer, N. (2006). Breaking the silence: Brain?computer interfaces (BCI) for communication and motor control. *Psychophysiology*, **43** (6), pp. 517–532.

Birbaumer, N. and Cohen, L. G. (2007). Brain-computer interfaces: communication and restoration of movement in paralysis. *The Journal of Physiology*, **579** (3), pp. 621–636.

Birbaumer, N., Ghanayim, N., Hinterberger, T., Iversen, I., Kotchoubey, B., Kübler, A., Perelmouter, J., Taub, E., and Flor, H. (1999). A spelling device for the paralysed. *Nature*, **398** (6725), pp. 297–298.

Bressler, S. L. (1995). Large-scale cortical networks and cognition. *Brain Research Reviews*, **20** (3), pp. 288–304.

Canolty, R. T., Edwards, E., Dalal, S. S., Soltani, M., Nagarajan, S. S., Kirsch, H. E., Berger, M. S., Barbaro, N. M., and Knight, R. T. (2006). High gamma power is phase-locked to theta oscillations in human neocortex. *Science (New York, N.Y.)*, **313** (5793), pp. 1626–8.

Chen, C.-W., K. Lin, C.-C., and J Ming, S. (2008). Hand orthosis controlled using brain-computer interface. *J of Med and Biol Eng*, **29**, pp. 234–241.

Chholak, P., Niso, G., Maksimenko, V. A., Kurkin, S. A., Frolov, N. S., Pitsik, E. N., Hramov, A. E., and Pisarchik, A. N. (2019). Visual and kinesthetic modes affect motor imagery classification in untrained subjects. *Scientific Reports 2019 9:1*, **9** (1), pp. 9838.

Craik, A., He, Y., and Contreras-Vidal, J. L. (2019). Deep learning for electroencephalogram (EEG) classification tasks: a review. *Journal of Neural Engineering*, **16** (3), pp. 031001.

Daly, J. J. and Wolpaw, J. R. (2008). Brain–computer interfaces in neurological rehabilitation. *The Lancet Neurology*, **7** (11), pp. 1032–1043.

Demiralp, T., Bayraktaroglu, Z., Lenz, D., Junge, S., Busch, N. A., Maess, B., Ergen, M., and Herrmann, C. S. (2007). Gamma amplitudes are coupled to theta phase in human EEG during visual perception. *International Journal of Psychophysiology*, **64** (1), pp. 24–30.

Dragoi, G. and Buzsáki, G. (2006). Temporal Encoding of Place Sequences by Hippocampal Cell Assemblies. *Neuron*, **50** (1), pp. 145–157.

Fries, P. (2005). A mechanism for cognitive dynamics: neuronal communication through neuronal coherence. *Trends in Cognitive Sciences*, **9** (10), pp. 474–480.

Guillot, A., Collet, C., Nguyen, V. A., Malouin, F., Richards, C., and Doyon, J. (2009). Brain activity during visual versus kinesthetic imagery: An fMRI study. *Human Brain Mapping*, **30** (7), pp. 2157–2172.

Guillot, A., Di Rienzo, F., Macintyre, T., Moran, A., and Collet, C. (2012). Imagining is Not Doing but Involves Specific Motor Commands: A Review of Experimental Data Related to Motor Inhibition. *Frontiers in human neuroscience*, **6**, pp. 247.

Gupta, A. S., van der Meer, M. A. A., Touretzky, D. S., and Redish, A. D. (2012). Segmentation of spatial experience by hippocampal θ sequences. *Nature neuroscience*, **15** (7), pp. 1032–9.

Halme, H.-L. and Parkkonen, L. (2016). Comparing Features for Classification of MEG Responses to Motor Imagery. *PLoS ONE*, **11** (12), pp. e0168766.

Halme, H.-L. and Parkkonen, L. (2018). Across-subject offline decoding of motor imagery from MEG and EEG. *Scientific Reports*, **8** (1), pp. 10087.

Hanakawa, T., Dimyan, M. A., and Hallett, M. (2008). Motor Planning, Imagery, and Execution in the Distributed Motor Network: A Time-Course Study with Functional MRI. *Cerebral Cortex (New York, NY)*, **18** (12), pp. 2775.

Harris, K. D., Csicsvari, J., Hirase, H., Dragoi, G., and Buzsáki, G. (2003). Organization of cell assemblies in the hippocampus. *Nature*, **424** (6948), pp. 552–556.

Hizanidis, J., Kouvaris, N. E., and Antonopoulos, C. G. (2015). Metastable and Chimera-like States in the C.Elegans Brain Network. *Cybernetics and Physics*, **4** (1), pp. 17–20.

Hwang, H.-J., Kim, S., Choi, S., and Im, C.-H. (2013). EEG-Based Brain-Computer Interfaces: A Thorough Literature Survey. *International Journal of Human-Computer Interaction*, **29** (12), pp. 814–826.

Jeneson, A. and Squire, L. R. (2012). Working memory, long-term memory, and medial temporal lobe function. *Learning & memory (Cold Spring Harbor, N.Y.)*, **19** (1), pp. 15–25.

Kai Keng Ang, Cuntai Guan, Sui Geok Chua, K., Beng Ti Ang, Kuah, C., Chuanchu Wang, Kok Soon Phua, Zheng Yang Chin, and Haihong Zhang (2009). A clinical study of motor imagery-based brain-computer interface for upper limb robotic rehabilitation. In *2009 Annual International Conference of the IEEE Engineering in Medicine and Biology Society*, IEEE, sep, pp. 5981–5984.

Kauhanen, L., Rantanen, P., Lehtonen, J. A., Tarnanen, I., Alaranta, H., and Sams, M. (2004). "sensorimotor cortical activity of tetraplegics during attempted finger movements" intention and imagery. *Biomed. Tech.*, **49**, pp. 59–60.

LaFleur, K., Cassady, K., Doud, A., Shades, K., Rogin, E., and He, B. (2013). Quadcopter control in three-dimensional space using a noninvasive motor imagery-based brain-computer interface. *Journal of neural engineering*, **10** (4), pp. 046003.

Lebon, F., Byblow, W. D., Collet, C., Guillot, A., and Stinear, C. M. (2012). The modulation of motor cortex excitability during motor imagery depends on imagery quality. *European Journal of Neuroscience*, **35**, pp. 323–331.

Lisman, J. E. and Jensen, O. (2013). The θ-γ neural code. *Neuron*, **77** (6), pp. 1002–16.

Llinás, R. and Ribary, U. (1993). Coherent 40-Hz oscillation characterizes dream state in humans. *Proceedings of the National Academy of Sciences of the United States of America*, **90** (5), pp. 2078–81.

Lotte, F., Congedo, M., Lécuyer, A., Lamarche, F., and Arnaldi, B. (2007). A review of classification algorithms for EEG-based brain–computer interfaces. *Journal of Neural Engineering*, **4** (2), pp. R1–R13.

Machado, S., Almada, L. F., and Annavarapu, R. N. (2013). Progress and Prospects in EEG-Based Brain-Computer Interface: Clinical Applications in Neurorehabilitation. *Journal of Rehabilitation Robotics*, **1** (1), pp. 28–41.

Machado, S., Araújo, F., Paes, F., Velasques, B., Cunha, M., Budde, H., Basile, L. F., Anghinah, R., Arias-Carrión, O., Cagy, M., Piedade, R., de Graaf, T. A., Sack, A. T., and Ribeiro, P. (2010). EEG-based brain-computer interfaces: an overview of basic concepts and clinical applications in neurorehabilitation. *Reviews in the neurosciences*, **21** (6), pp. 451–68.

Maris, E., van Vugt, M., and Kahana, M. (2011). Spatially distributed patterns of oscillatory coupling between high-frequency amplitudes and low-frequency phases in human iEEG. *NeuroImage*, **54** (2), pp. 836–50.

McFarland, D. J., Sarnacki, W. A., and Wolpaw, J. R. (2010). Electroencephalographic (EEG) control of three-dimensional movement. *Journal of Neural Engineering*, **7** (3), pp. 036007.

Meng, J., Zhang, S., Bekyo, A., Olsoe, J., Baxter, B., and He, B. (2016). Noninvasive Electroencephalogram Based Control of a Robotic Arm for Reach and Grasp Tasks. *Scientific Reports*, **6** (1), pp. 38565.

Moghimi, S., Kushki, A., Marie Guerguerian, A., and Chau, T. (2013). A Review of EEG-Based Brain-Computer Interfaces as Access Pathways for Individuals with Severe Disabilities. *Assistive Technology*, **25** (2), pp. 99–110.

Morash, V., Bai, O., Furlani, S., Lin, P., and Hallett, M. (2008). Classifying EEG signals preceding right hand, left hand, tongue, and right foot movements and motor imageries. *Clinical Neurophysiology*, **119** (11), pp. 2570–2578.

Mormann, F., Fell, J., Axmacher, N., Weber, B., Lehnertz, K., Elger, C. E., and Fernández, G. (2005). Phase/amplitude reset and theta-gamma interaction in the human medial temporal lobe during a continuous word recognition memory task. *Hippocampus*, **15** (7), pp. 890–900.

Müller-Putz, G. R., Scherer, R., Pfurtscheller, G., and Rupp, R. (2005). EEG-based neuroprosthesis control: A step towards clinical practice. *Neuroscience Letters*, **382** (1-2), pp. 169–174.

Murguialday, A. R., Aggarwal, V., Chatterjee, A., Cho, Y., Rasmussen, R., O'Rourke, B., Acharya, S., and Thakor, N. V. (2007). Brain-Computer Interface for a Prosthetic Hand Using Local Machine Control and Haptic Feedback. In *2007 IEEE 10th International Conference on Rehabilitation Robotics*, IEEE, jun, pp. 609–613.

Ono, T., Shindo, K., Kawashima, K., Ota, N., Ito, M., Ota, T., Mukaino, M., Fujiwara, T., Kimura, A., Liu, M., and Ushiba, J. (2014). Brain-computer interface with somatosensory feedback improves functional recovery from severe hemiplegia due to chronic stroke. *Frontiers in Neuroengineering*, **7**, pp. 19.

Pfurtscheller, G. and Lopes da Silva, F. (1999). Event-related EEG/MEG synchronization and desynchronization: basic principles. *Clinical Neurophysiology*, **110** (11), pp. 1842–1857.

Pfurtscheller, G. and Neuper, C. (1997). Motor imagery activates primary sensorimotor area in humans. *Neuroscience Letters*, **239** (2-3), pp. 65–68.

Ramos-Murguialday, A., Broetz, D., Rea, M., Läer, L., Yilmaz, Ö., Brasil, F. L., Liberati, G., Curado, M. R., Garcia-Cossio, E., Vyziotis, A., Cho, W., Agostini, M., Soares, E., Soekadar, S., Caria, A., Cohen, L. G., and Birbaumer, N. (2013). Brain-Machine-Interface in Chronic Stroke Rehabilitation: A Controlled Study. *Annals of neurology*, **74** (1), pp. 100.

Rayegani, S. M., Raeissadat, S. A., Sedighipour, L., Mohammad Rezazadeh, I., Bahrami, M. H., Eliaspour, D., and Khosrawi, S. (2014). Effect of Neurofeedback and Electromyographic-Biofeedback Therapy on Improving Hand Function in Stroke Patients. *Topics in Stroke Rehabilitation*, **21** (2), pp. 137–151.

Salmelin, R. and Hari, R. (1994). Spatiotemporal characteristics of sensorimotor neuromagnetic rhythms related to thumb movement. *Neuroscience*, **60** (2), pp. 537–550.

Sarac, M., Koyas, E., Erdogan, A., Cetin, M., and Patoglu, V. (2013). Brain Computer Interface based robotic rehabilitation with online modification of task speed. In *2013 IEEE 13th International Conference on Rehabilitation Robotics (ICORR)*, IEEE, jun, pp. 1–7.

Sauseng, P., Klimesch, W., Heise, K. F., Gruber, W. R., Holz, E., Karim, A. A., Glennon, M., Gerloff, C., Birbaumer, N., and Hummel, F. C. (2009). Brain Oscillatory Substrates of Visual Short-Term Memory Capacity. *Current Biology*, **19** (21), pp. 1846–1852.

Schnitzler, A., Salenius, S., Salmelin, R., Jousmäki, V., and Hari, R. (1997). Involvement of Primary Motor Cortex in Motor Imagery: A Neuromagnetic Study. *NeuroImage*, **6** (3), pp. 201–208.

Schwoebel, J., Boronat, C. B., and Branch Coslett, H. (2002). The man who executed "imagined" movements: evidence for dissociable components of the body schema. *Brain and Cognition*, **50**, pp. 1–16.

She, Q., Hu, B., Luo, Z., Nguyen, T., and Zhang, Y. (2019). A hierarchical semi-supervised extreme learning machine method for EEG recognition. *Medical & Biological Engineering & Computing*, **57** (1), pp. 147–157.

Siegel, M., Donner, T. H., and Engel, A. K. (2012). Spectral fingerprints of large-scale neuronal interactions. *Nature Reviews Neuroscience*, **13** (2), pp. 121–134.

Sirigu, A., Cohen, L., Duhamel, J. R., Pillon, B., Dubois, B., Agid, Y., and Pierrot-Deseilligny, C. (1995). Con-

gruent unilateral impairments for real and imagined hand movements. *NeuroReport*, **6**, pp. 997–1001.

Sirigu, A., Duhamel, J. R., Cohen, L., Pillon, B., Dubois, B., and Agid, Y. (1996). The mental representation of hand movements after parietal cortex damage. *Science*, **273**, pp. 1564–1568.

Skaggs, W. E., McNaughton, B. L., Wilson, M. A., and Barnes, C. A. (1996). Theta phase precession in hippocampal neuronal populations and the compression of temporal sequences. *Hippocampus*, **6** (2), pp. 149–172.

Solodkin, A., Hlustik, P., Chen, E. E., and Small, S. L. (2004). Fine Modulation in Network Activation during Motor Execution and Motor Imagery. *Cerebral Cortex*, **14** (11), pp. 1246–1255.

Sturm, I., Lapuschkin, S., Samek, W., and Müller, K.-R. (2016). Interpretable deep neural networks for single-trial EEG classification. *Journal of Neuroscience Methods*, **274**, pp. 141–145.

Tadel, F., Baillet, S., Mosher, J. C., Pantazis, D., and Leahy, R. M. (2011). Brainstorm: A user-friendly application for MEG/EEG analysis. *Computational Intelligence and Neuroscience*, **2011**.

Taulu, S. and Hari, R. (2009). Removal of magnetoencephalographic artifacts with temporal signal-space separation: Demonstration with single-trial auditory-evoked responses. *Human Brain Mapping*, **30** (5), pp. 1524–1534.

Varela, F., Lachaux, J.-P., Rodriguez, E., and Martinerie, J. (2001). The brainweb: Phase synchronization and large-scale integration. *Nature Reviews Neuroscience*, **2** (4), pp. 229–239.

Vaughan, T., Wolpaw, J., and Donchin, E. (1996). EEG-based communication: prospects and problems. *IEEE Transactions on Rehabilitation Engineering*, **4** (4), pp. 425–430.

Voytek, B., Canolty, R. T., Shestyuk, A., Crone, N. E., Parvizi, J., and Knight, R. T. (2010). Shifts in Gamma Phase–Amplitude Coupling Frequency from Theta to Alpha Over Posterior Cortex During Visual Tasks. *Frontiers in Human Neuroscience*, **4**.

Wolpaw, J. R. and McFarland, D. J. (1994). Multichannel EEG-based brain-computer communication. *Electroencephalography and Clinical Neurophysiology*, **90** (6), pp. 444–449.

Wolpaw, J. R. and McFarland, D. J. (2004). Control of a two-dimensional movement signal by a noninvasive brain-computer interface in humans. *Proceedings of the National Academy of Sciences*, **101** (51), pp. 17849–17854.

Wolpaw, J. R., McFarland, D. J., Neat, G. W., and Forneris, C. A. (1991). An EEG-based brain-computer interface for cursor control. *Electroencephalography and Clinical Neurophysiology*, **78** (3), pp. 252–259.

Yohanandan, S. A., Kiral-Kornek, I., Tang, J., Mshford, B. S., Asif, U., and Harrer, S. (2018). A Robust Low-Cost EEG Motor Imagery-Based Brain-Computer Interface. In *2018 40th Annual International Conference of the IEEE Engineering in Medicine and Biology Society (EMBC)*, IEEE, jul, pp. 5089–5092.